Half-space impedance Green's function for the Helmholtz equation

Yashraj Bhosale

December 15, 2019

1 INTRODUCTION

In this project, we consider the problem of wave scattering, commonly encountered in acoustics and electromagnetism. In the case of time harmonic behaviour of the incident waves, the physics of scattering can be studied using the Helmholtz equation

$$(\Delta + k^2 u(x)) = f(x) \tag{1.1}$$

where k is the wave number. Well-known formulations (Combined Field Integral Equations (CFIE)) exist for solving the scattering problem in an unbounded domain using boundary element methods, however one encounters a classical problem, when considering scattering from a body Ω in a half space (i.e. having an infinite wall at $y = 0$ with a certain boundary condition (fig. 1.1)). Two major approaches exist which avoid discretization of the boundary, each having their own pros and cons. In this project, we consider the implementation of a hybrid method derived from these two principal approaches [2], in the case of wave scattering in a 2D half space.

We begin by implementing a 2D Helmholtz equation solver, based on integral equations and a CFIE formulation.

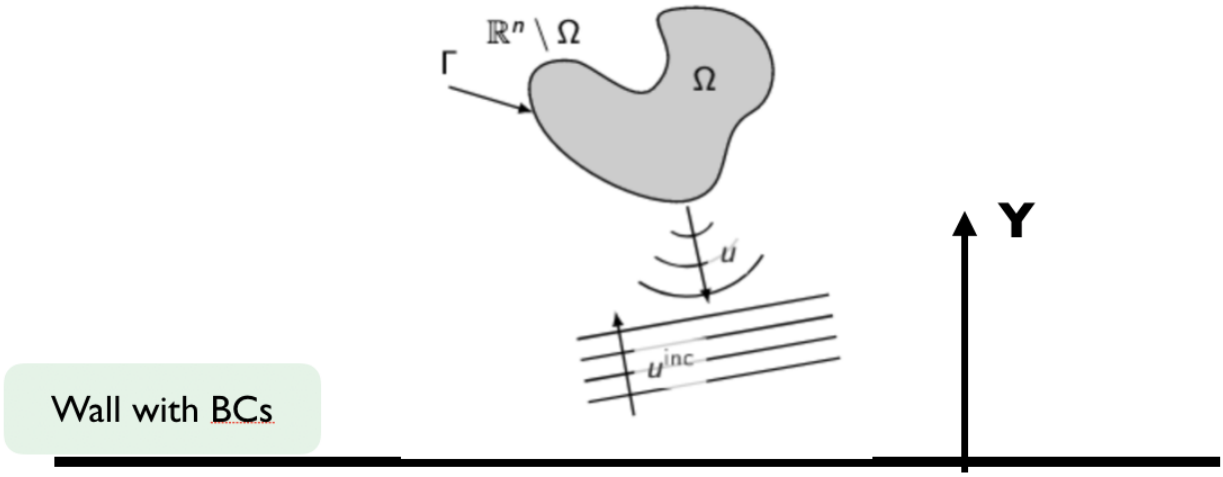

Figure 1.1: Half space scattering schematic: Incident waves u_{inc} are scattered from a body Ω in a half space $y > 0$. (credits: CS598APK notes)

2 2D Helmholtz equation: Greens function, IE formulation, validation and illustration

Consider the Helmholtz equation for a unit impulse source located at x_0 in an unbounded domain

$$\left(\Delta + k^2\right) g_k(\boldsymbol{x}) = \delta\left(\boldsymbol{x} - \boldsymbol{x}_0\right) \tag{2.1}$$

In 2D, the corresponding Greens function satisfying the Sommerfeld radiation condition is given by

$$g(x, x_0) = \frac{i}{4} H_0^{(1)}(k|x - x_0|) \tag{2.2}$$

where $H_0^{(1)}$ denotes the zeroth-order Hankel function of the first kind. Accordingly the single and double layer potentials for a certain charge density σ_y on a boundary are defined as:

$$\begin{aligned} S(x) &= \int g(x, y)\sigma(y)dy \\ D(x) &= \int n_y \frac{\partial}{\partial y} g(x, y)\sigma(y)dy \end{aligned} \tag{2.3}$$

We first consider the case of scattering of incident waves u_{inc} from a closed surface in an unbounded domain. Throughout this work, we will assume the body is 'sound soft' i.e a homogeneous Dirichlet condition $u_{tot} = u_{inc} + u_{scat} = 0$. We consider a standard CFIE representation as the solution for scattered field:

$$u(x) = D(x, y)\sigma(y) - i\alpha S(x, y)\sigma_y \tag{2.4}$$

where we set $\alpha = k$. Enforcing boundary conditions on the body surface we get (using jump relations):

$$\frac{\sigma}{2} + D\sigma - i\alpha S\sigma = -u_{inc} \tag{2.5}$$

a linear system, which is then solved for the source density using GMRES.

Since the layer potentials are singular when target and source coincide, for robust and accurate numerical quadrature on the surface using panels, we consider QBX [1]. In simple terms, we perform a local expansion (using Grafs addition theorem) of the singular kernel about a centre away from the source point fig. 2.1, and leverage the smoothness of the kernel in kernel evaluation. When the expansion centre distance from the panel r is set as half of

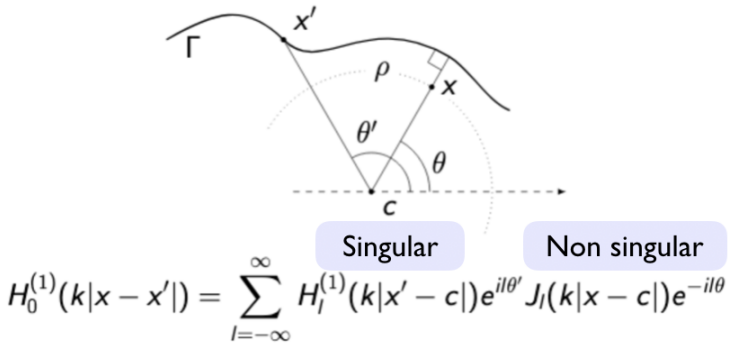

Figure 2.1: Illustration of Quadrature by Expansion (QBX) along with Grafs addition theorem (credits: CS598APK notes).

the panel length h, QBX converges with a controlled precision:

$$\epsilon = h^{p+1} + (0.25)^q \tag{2.6}$$

where p and q are the expansion order and number of Gaussian quadrature nodes on the panel, respectively.

Throughout our study, we consider the same cross shaped body parametrized as:

$$\begin{aligned} x(t) &= 1.1 + (1 + 0.2\cos(4t))\cos(t) \\ y(t) &= 2.0 + (1 + 0.2\cos(4t))\sin(t) \end{aligned} \tag{2.7}$$

For validation of the implementation, we consider the case of a monopole placed inside the body. The acoustic field induced at the body surface is used as a boundary condition for solving the external scattering problem. From the uniqueness of solution based on boundary values, the numerical solution should coincide with the analytical solution produced by the point source. Figure 2.2 shows the error plotted on a log scale in the domain (details in caption) and convergence of the solver with panel length. We recover the expected order of convergence as discussed above.

Figure 2.3 shows an illustration of the incident field from a source placed outside the body being scattered by the sound soft body.

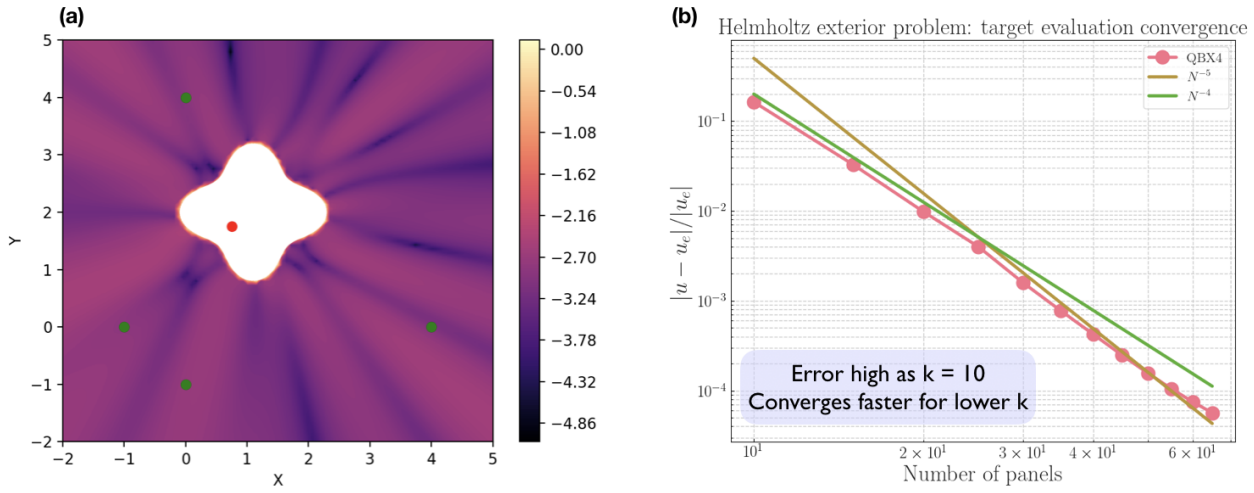

Figure 2.2: Convergence of IE solver for a monopole (red point) source placed in the body. (a) Error plotted on log scale for 30 panels, expansion order=4 and panel quadrature order=8. (b) Relative error convergence (L2 norm) for panel length h, evaluated at random points (green points) in the domain.

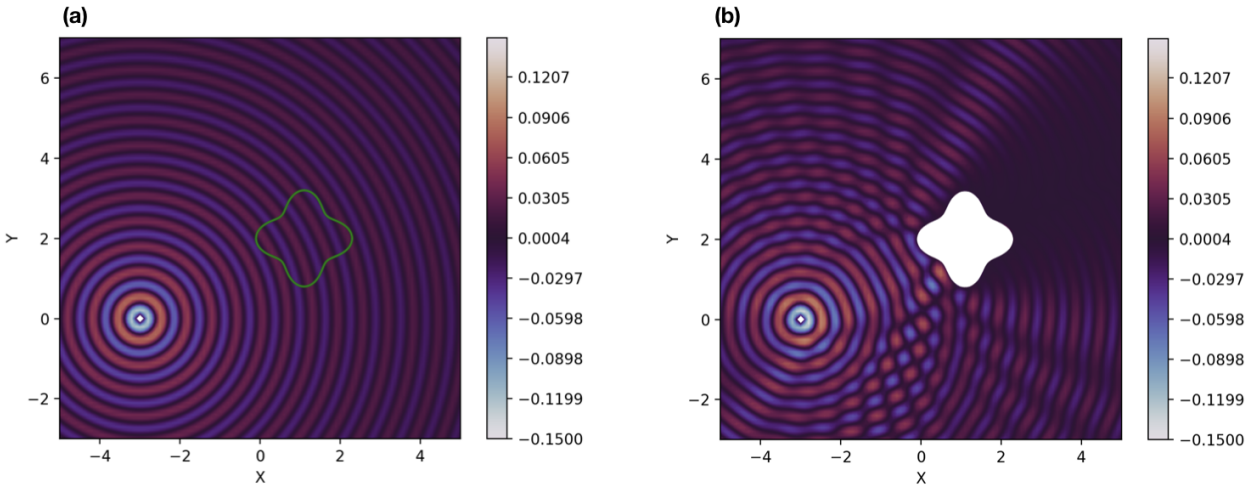

Figure 2.3: Scattering illustration: (a) Incident field (b) Total field after scattering from the body.

3 HALF SPACE PROBLEM

We now turn towards our main goal of developing the Greens function for a half space. For generic reasons, we assume the boundary condition on the wall ($y = 0$) to be of an impedance type i.e.

$$\frac{\partial u_{tot}}{\partial y} - i\alpha u_{tot} = 0 \tag{3.1}$$

We then discuss the two principal approaches to tackle this problem, followed by the hybrid method.

3.1 SOMMERFELD INTEGRAL REPRESENTATION

Consider the Greens function for the Helmholtz equation for an unbounded domain, with the source located at (x_0, y_0). The same function can be written as an integral of the Fourier modes:

$$g_k(\boldsymbol{x}, \boldsymbol{x}_0) = \frac{1}{4\pi^2} \int_{-\infty}^{\infty} \int_{-\infty}^{\infty} \frac{e^{i(\lambda_x(x-x_0)+\lambda_y(y-y_0))}}{\lambda_x^2 + \lambda_y^2 - k^2} d\lambda_x d\lambda_y \tag{3.2}$$

where λ_x and λ_y are the Fourier mode wavenumbers along x and y respectively. Integrating in λ_y using contour integration (a technique in complex analysis), the expansion can be written in terms of plane wave modes known as the Sommerfeld integral form as:

$$g_k(\boldsymbol{x}, \boldsymbol{x}_0) = \frac{1}{4\pi} \int_{-\infty}^{\infty} \frac{e^{-\sqrt{\lambda^2-k^2}|y-y_0|}}{\sqrt{\lambda^2-k^2}} e^{i\lambda(x-x_0)} d\lambda \tag{3.3}$$

where $\lambda(t) = t - i\tanh(t)$ for $t \in (-\infty, \infty)$. Similar to the above form, the Sommerfeld integral representation for single layer potential can be written as:

$$u(\boldsymbol{x}) = \frac{1}{4\pi} \int_{-\infty}^{\infty} \frac{e^{-\sqrt{\lambda^2-k^2}y}}{\sqrt{\lambda^2-k^2}} e^{i\lambda x} \widehat{\sigma}(\lambda) d\lambda \tag{3.4}$$

Using the above form and enforcing the impedance boundary condition of eq. (3.1) for all modes, the source density

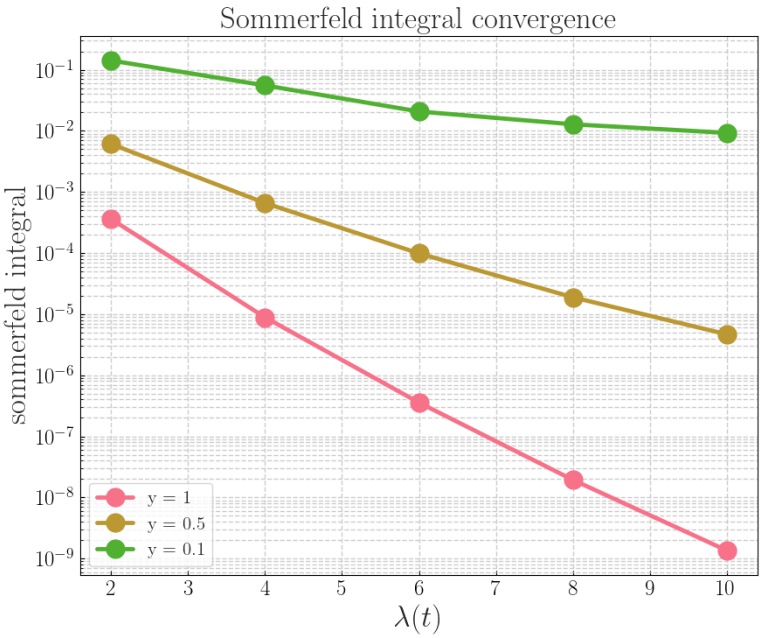

Figure 3.1: Convergence of the Sommerfeld integral for 3 different target locations (details in the code) for varying source distance from the wall. As can been seen, the convergence becomes worse as the source approaches the wall.

in the modal form can be written as:

$$\widehat{\sigma}(\lambda) = e^{-\sqrt{\lambda^2-k^2}y_0} e^{-i\lambda x_0} \left(\frac{\sqrt{\lambda^2-k^2} + i\alpha}{\sqrt{\lambda^2-k^2} - i\alpha} \right) \tag{3.5}$$

Substituting this back in the single layer potential yields:

$$u(\boldsymbol{x}) = \frac{1}{4\pi}\int_{-\infty}^{\infty} \frac{e^{-\sqrt{\lambda^2-k^2}(y+y_0)}}{\sqrt{\lambda^2-k^2}} e^{i\lambda(x-x_0)} \left(\frac{\sqrt{\lambda^2-k^2}+i\alpha}{\sqrt{\lambda^2-k^2}-i\alpha}\right) d\lambda \tag{3.6}$$

The above expression combined with the free space Greens function gives the full impedance Greens function for a half space, with a wall having impedance condition. However the above expression comes with two major issues. First, the term $e^{-\sqrt{\lambda^2-k^2}(y+y_0)}$ converges slowly if the target and the source are close to the wall (fig. 3.1). Second, the term $e^{i\lambda(x-x_0)}$ becomes large and oscillatory for larger distances between source and target, a fact common and unavoidable in Sommerfeld type representations. In short the representation is apt for far field interactions along y.

Next we discuss the second major approach, which may help us to resolve this issue.

3.2 Method of images

The method of images along with symmetry is well known in classical mathematics for application of homogeneous boundary conditions. Consider the case of a source placed at (x_0, y_0) and a wall at $y = 0$. A homogeneous Dirichlet condition can be imposed at the wall by placing an equal and opposite source at $(x_0, -y_0)$, while a homogeneous Nuemann condition can be imposed by placing the same source at $(x_0, -y_0)$. Similarly, for an impedance condition of eq. (3.1), one needs to place the same charge at (x_0, y_0) and a line of charges starting from the above location till $y = -\infty$ (see [3] for details).

Accordingly, for a source at (x_0, y_0), let us assume the scattered field takes the form:

$$u(\boldsymbol{x}) = \int_0^{\infty} g_k\left(\boldsymbol{x}, \boldsymbol{x}_0 - \left(2y_0+\eta\right)\widehat{\boldsymbol{y}}\right)\tau(\eta)\,d\eta \tag{3.7}$$

Writing the above expression in Sommerfeld integral type form:

$$u(\boldsymbol{x}) = \frac{1}{4\pi}\int_0^{\infty}\int_{-\infty}^{\infty} \frac{e^{-\sqrt{\lambda^2-k^2}(y+y_0+\eta)}}{\sqrt{\lambda^2-k^2}} e^{i\lambda(x-x_0)}\tau(\eta)\,d\lambda\,d\eta \tag{3.8}$$

Then enforcing the boundary condition of eq. (3.1), and simplifying the expression using some Laplace transform identities (see [2] for details), the scattered field can be written as:

$$u(\boldsymbol{x}) = g_k\left(\boldsymbol{x}, \boldsymbol{x}_0 - 2y_0\widehat{\boldsymbol{y}}\right) + 2i\alpha\int_0^{\infty} g_k\left(\boldsymbol{x}, \boldsymbol{x}_0 - \left(2y_0+\eta\right)\widehat{\boldsymbol{y}}\right) e^{i\alpha\eta}\,d\eta \tag{3.9}$$

In the above expression, the source density is of oscillatory nature while the decay in the integral comes only from the Greens function. To overcome this, one can complexify η using contour integration and rewrite the expression as:

$$u(\boldsymbol{x}) = g_k\left(\boldsymbol{x}, \boldsymbol{x}_0 - 2y_0\widehat{\boldsymbol{y}}\right) - 2\alpha\int_0^{\infty} g_k\left(\boldsymbol{x}, \boldsymbol{x}_0 - \left(2y_0+i\eta\right)\widehat{\boldsymbol{y}}\right) e^{-\alpha\eta}\,d\eta \tag{3.10}$$

The above expression now shows exponential decay, thus making the integral evaluation easier. However as a side effect now, the Greens function part of the integrand lies in the complex plane and shows spatial dependence of the singularity, relative to the target and source locations (fig. 3.2). This makes use of a generic quadrature scheme problematic.

Next, we demonstrate a hybrid representation, combining the pros and eliminating the cons of both the methods.

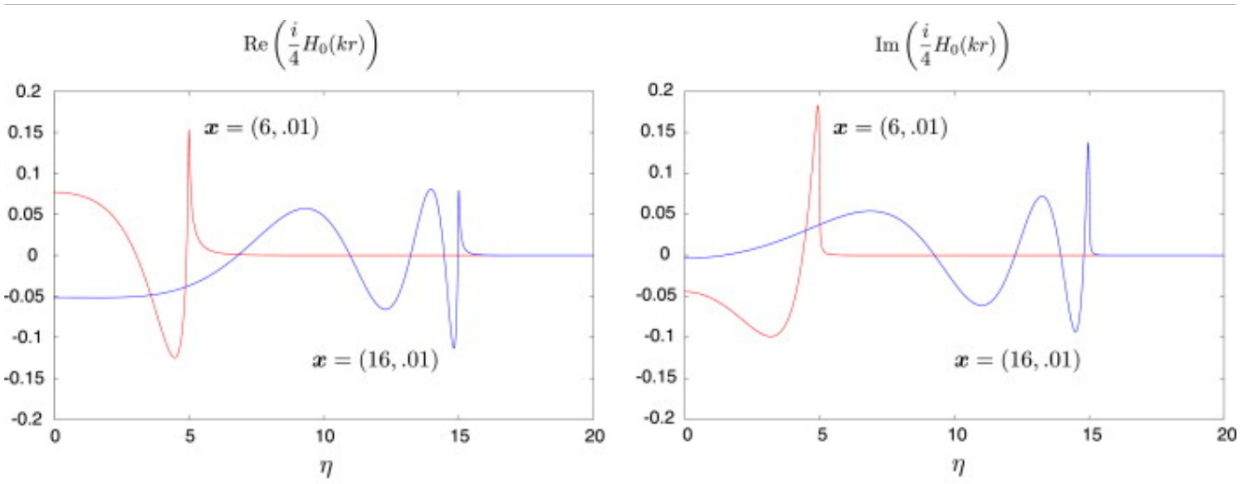

Figure 3.2: For $k = 1$ and source location $(1, 0.01)$, the plot shows the behavior of the singularity of and its dependence on the lateral location of the source and target.

3.3 A HYBRID APPROACH

Consider the image base representation of eq. (3.9). Now splitting the integral into near and far field components:

$$\begin{aligned} u(\boldsymbol{x}) &= g_k\left(\boldsymbol{x}, \boldsymbol{x}_0 - 2y_0\hat{\boldsymbol{y}}\right) \\ &+2i\alpha\left(\int_0^C g_k\left(\boldsymbol{x}, \boldsymbol{x}_0 - (2y_0 - \eta)\hat{\boldsymbol{y}}\right) e^{i\alpha\eta} d\eta + \int_C^\infty g_k\left(\boldsymbol{x}, \boldsymbol{x}_0 - (2y_0 - \eta)\hat{\boldsymbol{y}}\right) e^{i\alpha\eta} d\eta\right) \end{aligned} \tag{3.11}$$

where C is parameter of choosing (chosen = 1, based on [2]). Now the third term on RHS or the far field form has

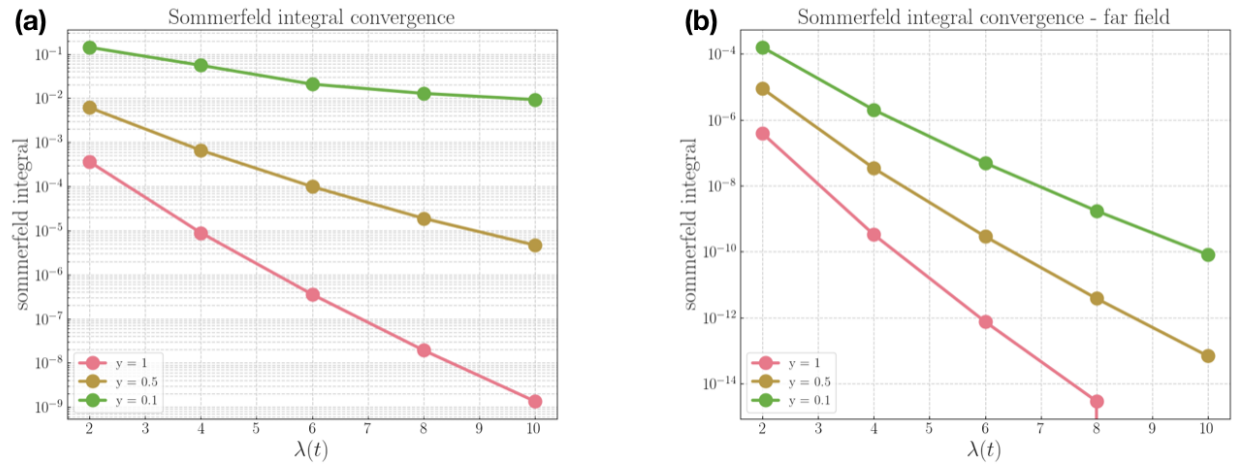

Figure 3.3: For a source at (0, 2), $k = 10.4$, $\alpha = 2.04$ and wall at y=0, convergence of (a) traditional Sommerfeld integral (b) far field Sommerfeld integral, for varying target locations.

closed-form Sommerfeld integral representation:

$$\int_C^\infty g_k\left(\boldsymbol{x}, \boldsymbol{x}_0 - 2y_0\hat{\boldsymbol{y}} - \eta\hat{\boldsymbol{y}}\right) e^{i\alpha\eta} d\eta = \frac{1}{4\pi}\int_{-\infty}^{\infty} \frac{e^{-\sqrt{\lambda^2-k^2}(y+y_0)}}{\sqrt{\lambda^2-k^2}} \frac{e^{-(\sqrt{\lambda^2-k^2}-i\alpha)c}}{\sqrt{\lambda^2-k^2}-i\alpha} e^{i\lambda(x-x_0)} d\lambda \tag{3.12}$$

The above expression has a term $e^{-(\sqrt{\lambda^2-k^2}-i\alpha)C}$, which decays exponentially irrespective of the location of the target or source, thus making the integral converge rapidly. Figure 3.3 demonstrates this fact, with the far field Sommerfeld integral converging rapidly when compared to the traditional Sommerfeld integral. The second term on the RHS is then integrated numerically on dyadic intervals. Further details on quadrature can be found in [2]. Figure 3.4

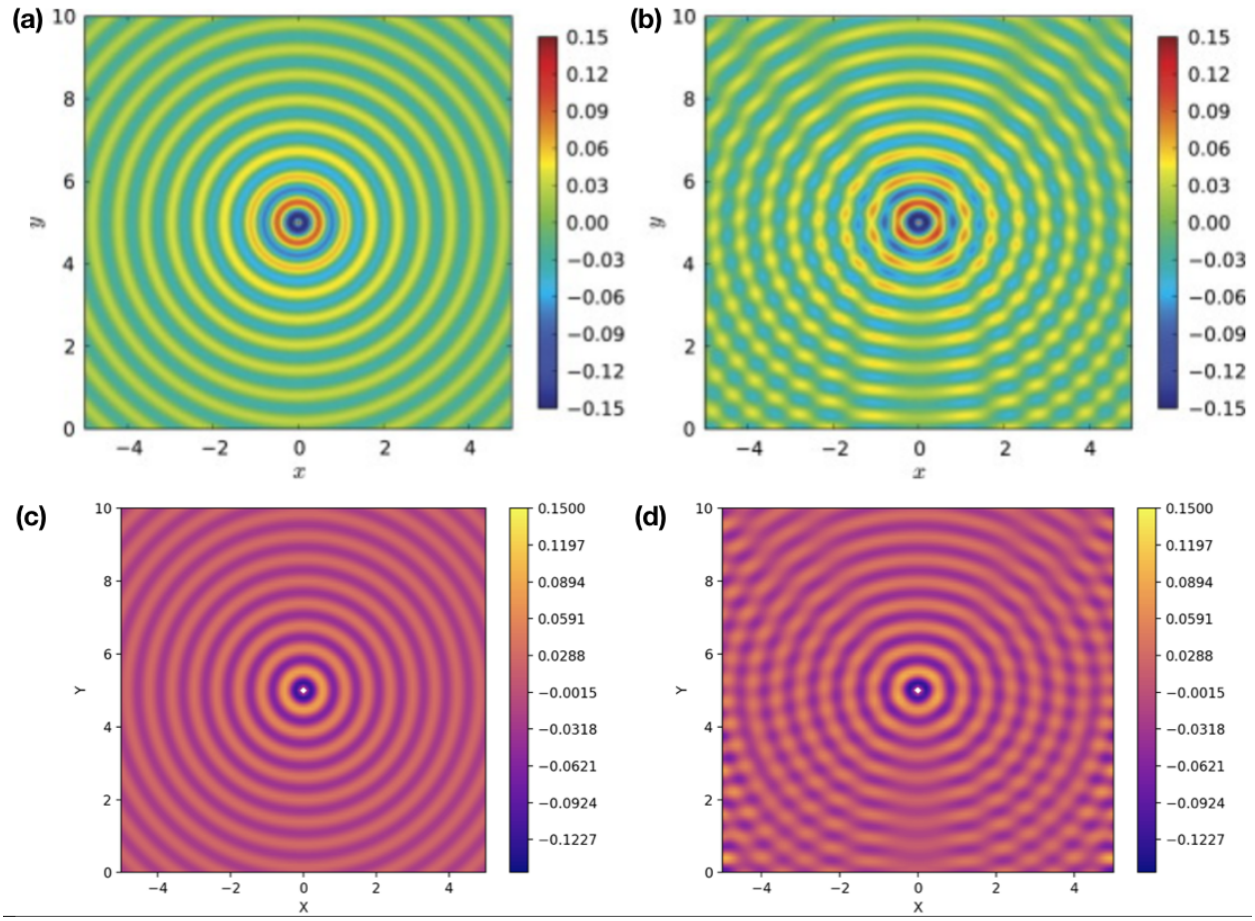

Figure 3.4: For a source at (0, 5), $k = 10.4$, $\alpha = 2.04$ and wall at y=0, (a) and (b) illustrate the incident and scattered Greens function, respectively from [2] while (c) and (d) illustrate the corresponding fields from our implementation. We see qualitative agreement between the two.

demonstrates the comparison for the scattered hybrid Greens function, between [2] and our own implementation, and shows qualitative agreement between the two.

We next insert this modified Greens function in our Helmholtz scattering IE solver and observe the scattered fields from the body in a half space, with waves incident from a source at (-2, 2). Figure 3.5 illustrates the comparison between scattered fields from our implementation and that of [2]. Near smaller horizontal target–source separation and near the body, we see qualitative agreement. For larger lateral separation, we see large oscillating values which we believe is due to the $e^{i\lambda(x-x_0)}$ term. Figure 3.6 shows the convergence of the scattered field at 3 random points near the scatterer, which shows the expected order.

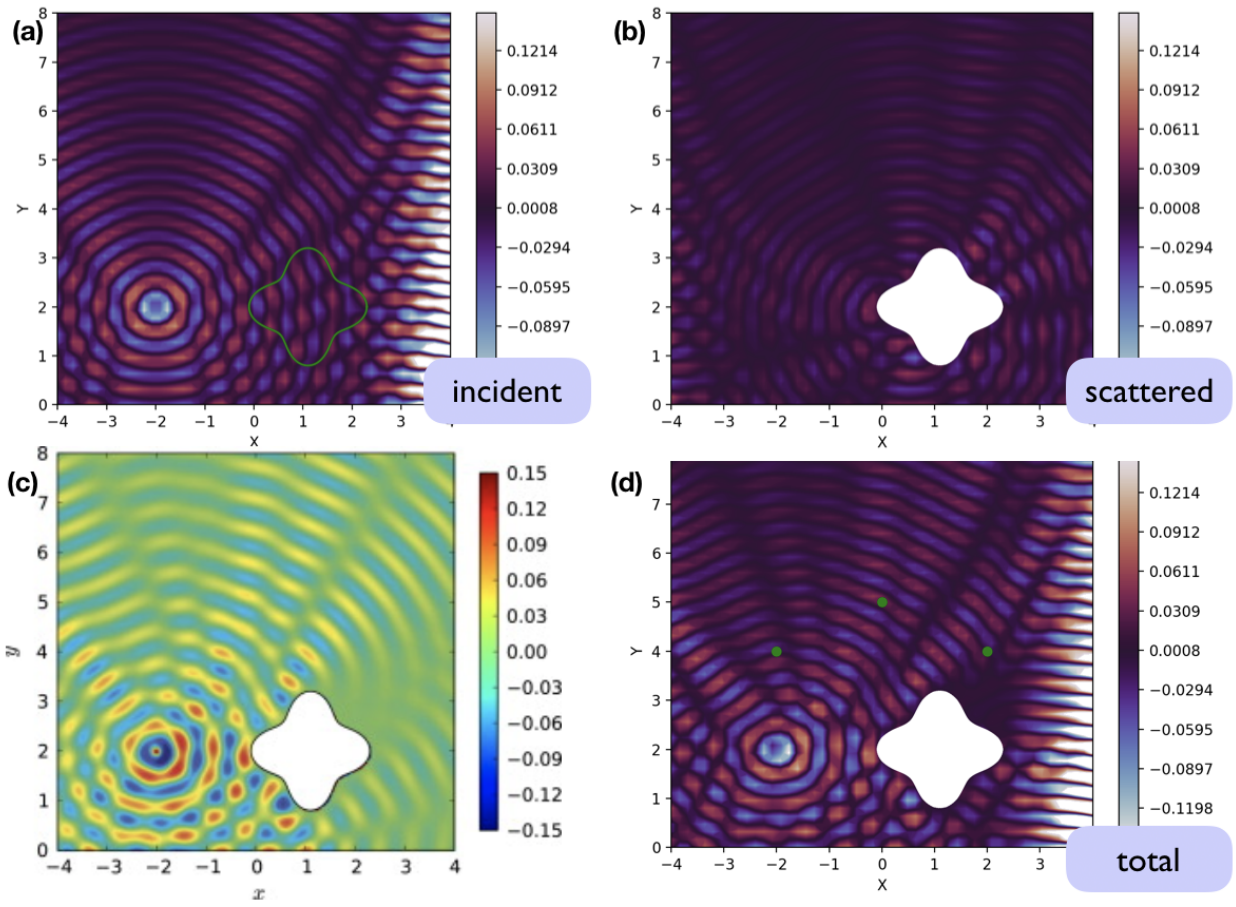

Figure 3.5: For a source at (-2, 2), $k = 10.4$, $\alpha = 2.04$ and wall at y=0, (a), (b) and (d) illustrate the incident, scattered and total fields from our implementation. (c) Illustration of the scattered field from [2]. We see qualitative agreement between the two.

4 Conclusion

To approach the acoustic scattering problem, an IE solver based on CFIE representation for Helmholtz equation using QBX for layer potential quadrature was successfully implemented and validated in Python. Two major approaches of developing a half space Greens function, Sommerfeld integral and method of images were discussed, along with their pros and cons. Finally, a hybrid approach, combining the two was implemented for scattering in a half space and results were compared with those of [2]. Qualitative agreement was observed between the two. What remains further is reducing the complexity of the implementation using FMM for image charges, as well as understand how FMM works in the case of QBX.

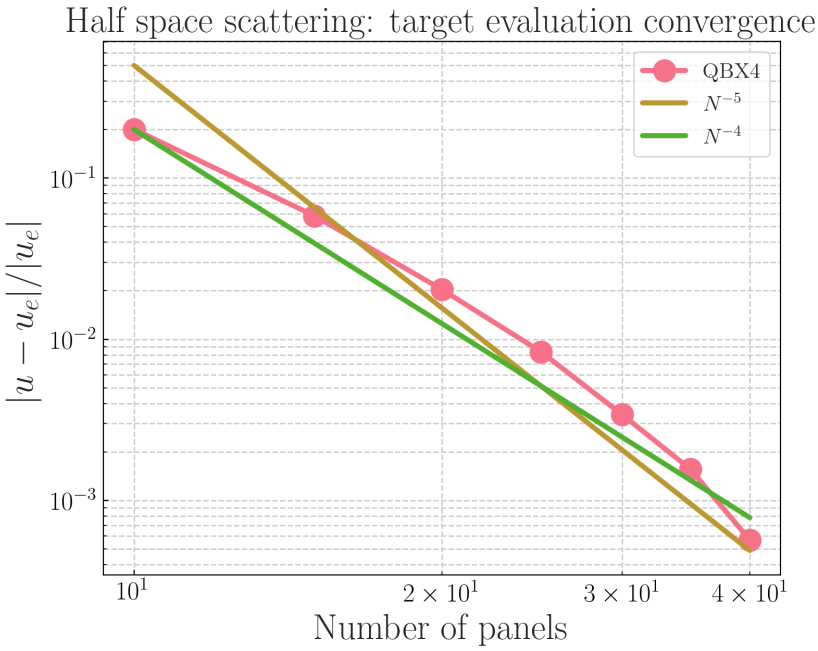

Figure 3.6: For a source at (-2, 2), $k = 10.4$, $\alpha = 2.04$ and wall at y=0, convergence at three random points (plotted in fig. 3.5).

REFERENCES

[1] Klockner, A., Barnett, A., Greengard, L., and O'Neil, M. (2013). Quadrature by expansion: A new method for the evaluation of layer potentials. *Journal of Computational Physics*, 252:332–349.

[2] O'Neil, M., Greengard, L., and Pataki, A. (2014). On the efficient representation of the half-space impedance green's function for the helmholtz equation. *Wave Motion*, 51(1):1–13.

[3] Taraldsen, G. (2005). The complex image method. *Wave Motion*, 43(1):91–97.